Bioassays and field observations revealed complex and different genetic bases in Pestalotiopsis and circular leaf fall disease in Hevea brasiliensis

Muhamad Rizqi Darojat, Alchemi Putri Juliantika Kusdiana, Pascal Montoro, David Lopez, Fetrina Oktavia, Sigit Ismawanto, Sudarsono Sudarsono

HAL Id: hal-04777831

https://hal.inrae.fr/hal-04777831v1

Submitted on 12 Nov 2024

Bioassays and field observations revealed complex and different genetic bases in *Pestalotiopsis* and circular leaf fall disease in *Hevea brasiliensis*

Muhamad Rizqi Darojat [a,1], Alchemi Putri Juliantika Kusdiana [a,1], Pascal Montoro [b,c,1,*], David Lopez [b,c], Fetrina Oktavia [a], Sigit Ismawanto [a], Sudarsono Sudarsono [d]

[a] *Indonesian Rubber Research Institute, Sembawa, Banyuasin, South Sumatra 30953, Indonesia*
[b] *CIRAD, UMR AGAP Institut, Montpellier F-34398, France*
[c] *UMR AGAP Institut, Univ Montpellier, CIRAD, INRAE, Institut Agro, Montpellier F-34398, France*
[d] *Department of Agronomy and Horticulture, Faculty of Agriculture, IPB University, Bogor 16680, Indonesia*

ABSTRACT

Circular leaf fall disease (LFD) has been spreading in South-East Asia since 2018. This disease has been considered to be the most important factor that influences natural rubber yield. After identifying *Pestalotiopsis* as the causal agent of circular LFD, several studies reported the potential involvement of another primary agent. The aim of the present study was to understand the genetic basis of the infection caused by *Pestalotiopsis* in bioassays under controlled conditions and field observations of circular disease. Individuals from a biparental population resulting from a cross between clones PB 260 and SP 217 were phenotyped. The symptoms on leaves inoculated with two isolates of *Pestalotiopsis* in bioassays and natural infection in the field were found to be identical. Of the two *Pestalotiopsis* isolates, PE-001 produced a lesion with a larger average diameter in the population compared to PE-002. The severity of the disease observed in the field increased regularly for three years. Bioassays with *Pestalotiopsis* isolates and field observations revealed no correlation. The classification of genotypes has made it possible to identify classes with both small lesion diameters and low disease severity. Heritability of the lesion diameter was found to be much higher in bioassays than heritability of disease severity observed in the field. The QTLs detected differed between bioassay isolates and field observations. The latter QTLs did not remain stable over time and were no longer detected when disease severity increased in March 2023. The QTLs are associated with long chromosomal regions harbouring many genes associated with the gene ontology terms "molecular function" and "biological process", the latter being associated with the response to biotic factors. The results of the bioassays confirmed *Pestalotiopsis* as the agent causing the symptoms of circular disease. This disease has a complex genetic basis which evolves over time.

1. Introduction

Hevea brasiliensis is the main commercial source of natural rubber (NR). Leaf-fall diseases (LFD) cause defoliation in rubber plantations, which affect NR production (Priyadarshan, 2017). In 2017, the first outbreak of a new disease, called circular LFD by the pathologist group of the International Rubber Research and Development Board on 17 December 2022, occurred in North Sumatra (Junaidi et al., 2018). Today, this disease is encountered in all provinces of Indonesia, as well as in Malaysia and Thailand (Aliya et al., 2022; Pornsuriya et al., 2020). NR yield losses have been estimated at 10–30 % in these producer

countries, making the fight against circular LFD disease a priority for governments (Rodesuchit, 2020).

The development of circular LFD is influenced by environmental factors, including relative humidity, rainfall, wind speed, and exposure to sunlight (Kusdiana et al., 2021). The rapid spread of circular LFD was thought to be related to climate change associated with El Niño and La Niña (Febbiyanti, 2020). Different pathogens may cause circular LFD, and *Fussicoccum* sp. was originally suggested to be the causal agent of circular LFD (Febbiyanti et al., 2018). However, Koch's Postulate analysis revealed that *Colletotrichum* spp. could be the main cause of the circular LFD and *Pestalotiopsis* a secondary pathogen (Rodesuchit, 2020).

Other studies reported that a combination of pathogens such as *Colletotrichum siamense* and *Pestalotiopsis jesteri* could be the causal agents of the disease (Aliya et al., 2022; Guevara et al., 2022; Thaochan et al., 2022). Studies using single DNA fragment (ITS) or multiple fragments (ITS, TUB, and TEF) molecular markers revealed that *Pestalotiopsis* was the main pathogen responsible for circular LFD (Febbiyanti and Fairuza, 2019; L. Li et al., 2021a; Pornsuriya et al., 2020).

Several *Pestalotiopsis* species have been identified on infected rubber leaves. *Pestalotiopsis*, *Pseudopestalotiopsis*, and *Neopestalotiopsis* are members of the *Pestalotiopsidaceae* family in the *Ascomycota* phylum (Maharachchikumbura et al., 2014). The pathogen infects green leaves from stage B (pale-green leaf) on, and visible circular LFD symptoms are round brown spots on mature leaves from stage D on (Halle and Martin, 1968). The infected leaf can change colour to yellow or orange (Kusdiana et al., 2020). Later, a total of nine species were identified on leaves showing this symptom: *Neopestalotiopsis cubana* and *Neopestalotiopsis formicarum* (Pornsuriya et al., 2020), *Pseudopestalotiopsis theae* ((Permana and Diyasti, 2022), *Pseudopestalotiopsis coccos* and *Neopestalotiopsis cubana* (Febbiyanti et al., 2022), *Pestalotiopsis jester* (Aliya et al., 2022), *Pestalotiopsis microspore* (Kusdiana et al., 2020), *Neopestalotiopsis aotearoa* (L. Li et al., 2021b), *Pseudopestalotiopsis simitheae* (Febbiyanti and Fairuza, 2019), and *Neopestalotiopsis saprophytica* (Darojat et al., 2023).

Characterising *Pestalotiopsis* species is necessary to understand their role in the pathogenic mechanism involved in circular LFD, but is nevertheless challenging. Fungal pathogens have also been isolated on infected leaves with circular symptoms and identified and characterised using morphological and molecular analyses (Febbiyanti et al., 2022; Kusdiana et al., 2020; B. Li et al., 2021; Pornsuriya et al., 2020). *Pestalotiopsis* was thought to act as an opportunistic pathogen that caused secondary infections on rubber tree leaves (Aliya et al., 2022). Among the four races isolated from *Neopestalotiopsis saprophytica*, isolate P-212 was found to be the most virulent (Darojat et al., 2023). Another isolate found in rubber clone GT1 was identified using the ITS DNA fragment (Kusdiana et al., 2020). These two isolates led to bioassays on detached leaves. However, bioassays and field observations produced contradictory results. Bioassays revealed that clones IRR 39 and PB 260 are susceptible to the circular LFD, while clone SP 217 showed moderate resistance in the bioassay (Darojat et al., 2023). By contrast, field observations showed that clone IRR 39 is moderately resistant to the disease (Kusdiana et al., 2020). Interestingly, clones RRIC 100 and IRR 112 were resistant to circular LFD (Damiri et al., 2022).

Disease resistance in plants is controlled by multiple genes and multiple molecular mechanisms. Both qualitative and quantitative disease resistance is influenced by major genes plus by the minor effects of multiple genes. In rubber, genetic studies have been conducted on the South American Leaf Blight (SALB) and Corynespora Leaf Fall (CLF) diseases. In the case of SALB, eight QTLs were associated with resistance in controlled conditions (Lespinasse et al., 2000), while field observations revealed one major QTL located on the linkage group g13 (Le Guen et al., 2003). In the case of CLF, genetic analysis of sensitivity to *Corynespora cassiicola* was carried out using exudates from culture filtrates (Tran et al., 2016) and revealed complex determinism involving six QTLs located on five chromosomes.

The aim of the present study was thus to decipher the genetic base of *Pestalotiopsis* by comparing bioassays and field observations of circular LFD. Phenotyping was carried out on an F1 population, containing 201 individuals produced by hand pollination between rubber clones PB 260 and SP 217, and control clones (Ismawanto et al., 2024). Bioassays were carried out using the two virulent isolates P212 and GT1, renamed PE-001 and PE-002 in this paper. A genetic linkage map based on SSR and SNP markers developed by Ismawanto and collaborators was used in this study (Ismawanto et al., 2024). This is the first genetic study of circular LFD in which field observation revealed a different genetic basis than when *Pestalotiopsis* isolates were inoculated under control conditions. These results pave the way for further research into understanding the disease, resistance mechanisms, and breeding clones resistant to circular LFD.

2. Materials and methods

2.1. Plant material

A progeny comprising 257 individuals was obtained from the cross between clones PB 260 x SP 217. The parent clones PB 260 and SP 217 were respectively susceptible and moderately resistant to *Pestalotiopsis* (Darojat et al., 2023). Seedlings of this progeny were planted in a seedling collection, then propagated by grafting and preserved in a budwood garden. One hundred and sixty-nine genotypes were used for the bioassay in the study as well as five rubber clones including clones PB 260, SP 217, RRIC 100, IRR 112 and IRR 39.

A small-scale clone trial (hereafter SSCT1) was established in 2016 at the Indonesian Rubber Research Institute (GPS coordinates: 2°58'13.2" S 104°28'51.1" E). The trial consists of 201 genotypes from the progeny PB 260 x SP 217 plus eight control clones including the parent clones (PB 260, SP 217) and other recommended clones (AVROS 2037, GT1, IRR 112, IRR 39, PR 261, and RRIC 100). The trial is organised in five blocks (replicates) of two trees per genotype (duplicates) for each replicate.

2.2. Isolation of Pestalotiopsis

Infected rubber tree leaves with visible circular spot symptoms were taken from the PB 260 x SP 217 population planted in the budwood collection, placed in individual plastic bags and brought to the laboratory. Fungal pathogens were isolated following the method described by Kusdiana and collaborators (Kusdiana et al., 2020). Approximately 5 mm pieces of infected leaves were cut out and sterilised through immersion in 1 % sodium hypochlorite for 30 sec, followed by 70 % ethanol for 30 sec, and then rinsed three times with sterile distilled water. The leaf samples were then dried on sterile tissue paper and placed in potato dextrose agar (PDA) medium, incubated at 25±2 ºC for two weeks until acervuli appeared. In addition, all the isolates were purified using the single spore method (Solarte et al., 2018). Isolate P-212 has already been subject of morphological and molecular characterisation using ITS primer, it was identified as *Neopestalotiopsis* sp. (Darojat et al., 2023) and is renamed in this paper PE-001. The same procedure was used for the isolation of one isolate from clone GT1, called PE-002 in this paper (Kusdiana et al., 2020).

2.3. Bioassay with two Pestalotiopsis isolates

Samples of healthy leaves from the progenies in the F1 seedling collection were collected at stage C (i.e. 15 days old) according to Fang's recommendations (Fang et al., 2016). The leaf samples were cleaned under running water, wiped with 70 % ethanol, and then air dried. Before inoculation, the abaxial side of the sampled leaves was wounded with a sterile needle three times in two different places on the leaf. Three leaves per genotype were put in individual plastic boxes, and the petioles were covered with moist sterile cotton. The box was then kept in a room at 25±2 ºC with roughly 100 % relative humidity until use. All the progeny individuals were tested using the two isolates, PE-001 and PE-002. Seven to ten-day-old mycelium plugs measuring five millimetres in diameter were used to inoculate the leaves. The experiment was conducted in a completely randomised design with three replications. Resistance was evaluated by measuring the diameter of the lesion (mm) seven days after inoculation. The leaves were scanned at 400 dpi (Canon E510), and the lesion diameter was measured using ImageJ software (Schneider et al., 2012).

2.4. Field observations of circular leaf fall disease

Each individual tree in the small-scale clone trial SSCT1 was

monitored in February 2020, September 2021, January 2022, August 2022 and March 2023. Scoring was based on the condition of the canopy and the main symptoms observed on attached leaves were confirmed on fallen leaves. Round brown spots were considered as symptoms of circular LFD. A score of 0–4 was attributed to each tree as follows:

- Score 0: no defoliation and no symptoms on leaves,
- Score 1: 4–20 % of defoliation and symptoms on a few leaves,
- Score 2: 21–50 % of defoliation and symptoms on a few leaves,
- Score 3: 51 %-75 % of defoliation and symptoms on most leaves
- Score 4: 76–100% of defoliation and symptoms on most leaves

Based on the score, the percentage of disease severity was calculated using the formula established by Chaube and Singh (Chaube and Singh, 1991):

$$Disease\ severity = \frac{\sum\limits_{i-1}^{n}(n.v)}{Z.N}x \quad 100\%$$

where n is the number of plants with a scale -v, v is the scale to-i, Z is the highest score, and N is the number of plants observed.

2.5. Data analysis and classification of variables

All calculations were made using Excel (Microsoft Office 2019, Washington, USA) and XLSTAT (Addinsoft 1995–2024, Denver, USA). For the diameter of the lesions in the bioassays, LS-means were calculated by ANOVA using the average diameter of the lesions measured on every leaf. Genotypes were classified from 1 to 4 for low, medium-low, medium-high and high lesion diameters using quantiles (0–25, 25–50, 50–75 and 75–100). For disease severity, the frequency was calculated using the formula (Hunter, 1983):

$$Frequency = \frac{\sum\limits_{i-1}^{n}n.v}{N}x \quad 100\%$$

where n is the number of plants with a scale -v, v is the scale to-i, and N is the number of plants observed. Quantile classification was performed at each observation date. The sum of classes was divided by the number of observations (5) and discrete classes were then determined.

2.6. Conformity test and construction of a high-density genetic map

The conformity of trees in the SSCT1 trial and the construction of the genetic map are detailed in a previous study(Ismawanto et al., 2024). Genotyping was carried out using a set of 8 microsatellite markers (Cubry et al., 2014). The profiles were compared with the original genotypes planted in the seedling collection. Genotypes with erroneous profiles were excluded from the analysis.

A high-density map was previously generated by genotyping-by-sequencing (Ismawanto et al., 2024). This GBS method was developed at the AGAP Regional Genotyping Platform (Mournet et al., 2020). A *Pst*I-*Mse*I genomic library was built using 200 ng of DNA per sample. After SNP calling (105 993 SNPs), filtering and matrix correction, the genetic map was constructed using 273 SSR markers identified by Tran and collaborators (Tran et al., 2016), and 3 106 new SNP markers (Ismawanto et al., 2024). This total length of this map is 2 046.294 cM for 18 linkage groups from 88.259 to 144.913 cM with marker density ranging from 0.533 to 2.522 cM.

2.7. Heritability and QTL detection

Genotype-level heritability (hf) and BLUP values per genotype were calculated with R Studio (version 4.2.1) using the lme4 package for the mixed model equation (Bates et al., 2015). The broad sense heritability

at the genotype level is defined as:

$$\frac{Vg}{\left(Vg + \frac{Ve}{n}\right)}$$

Where hf is the heritability at genotype level, Vg the genetic variance, Ve the environmental variance and n the number of individuals.

BLUP values were extracted from the blup table and used for QTL detection with MapQTL6 (Kyazma B.V. 1996–2011, Wageningen, Netherlands).

The linear model used was: $Y_{ijk} = \mu + G_i + b_j + D_{ij} + \epsilon_{ijk}$

where μ is the constant term, G the genetic effect, b the block effect, D the genotype by block interaction and ϵ the residual.

Three data files were loaded to perform QTL analysis: file.qua, file. loc and file.map. A non-parametric Kruskal-Wallis (KW) test was performed because the diameters of the lesions and disease severity calculated from the score observed in the SSCT1 trial did not follow a normal distribution. QTLs were selected in region with a Kruskal-Wallis value (K) higher than 10 with a p-value lower than 0.0005.

2.8. Genome sequence and identification of genes underlying the QTLs

The clone PB 260 genome assembly was obtained using PacBio HiFi technology and the SMRT (Single Molecule Real Time) sequencing platform. The draft assembly comprises 395 high-quality contigs representing 1.6 Gb. This assembly is publicly available at https://zenodo.org/doi/10.5281/zenodo.10281548. The 58,062 full-length cDNA sequences of clone Reyan 7–33–97 (Tang et al., 2016) were aligned on the assembly using minimap2 (Li, 2018), followed by bedToGenePred then genePredToGtf from UCSC Kent tools v385 to characterise the gene coding landscape of the QTLs. These tools were used to refine alignment into a proper intron/exon structure in the gtf format (Kent et al., 2002). Finally, the overlap between predicted genes and QTLs was detected using Bedtools v2.30.0 (Quinlan and Hall, 2010). In order to perform Gene Ontology (GO) term enrichment in the QTL regions, an update of Reyan 7–33–97 functional annotation was performed using Inter-ProScan-5.67–99.0 (Jones et al., 2014) on the predicted protein sequences. Functional enrichment was assessed in the QTL regions using GofuncR package version 1.22.2 (Grote 2024) using hypergeometric test that does statistical test on the frequency of terms in a subset versus their frequency in the whole predicted proteome defined as the background level. If the frequency of terms among the subset is different than what should be randomly found, then a p value is attributed to the term. The hypergeometric test and a family wise discovery rate were applied on the raw p-value which lowers false prediction rate. GO terms with a corrected p-value, i.e. family-wise error rate (FWER) below 0.05 were considered significant.

3. Results

3.1. Description of the symptoms

Circular LFD is widely observed on the leaves of many rubber clones at all stages, including immature, mature stages, as well as in budwood and seedling collections. The disease infects young leaves (stage A or B), and severe infection can cause discolouration of mature leaves, leaf drop and a sparse tree canopy (Fig. 1, photos A and B). The symptoms appeared in the form of circular spots measuring 10–20 mm in diameter and of a brown or grey necrotic lesion, with more than two spots per leaf (Fig. 1, C). The bioassay performed in the present study produced symptoms similar to those observed produced by natural infection under different levels of resistance in the two parent clones (Fig. 1, photos D to G). The virulence of the isolates influenced the level of clonal resistance. In the present study, isolate PE-001 produced a lesion with a larger diameter than isolate PE-002 (Fig. 1, photos D and E and Supplementary
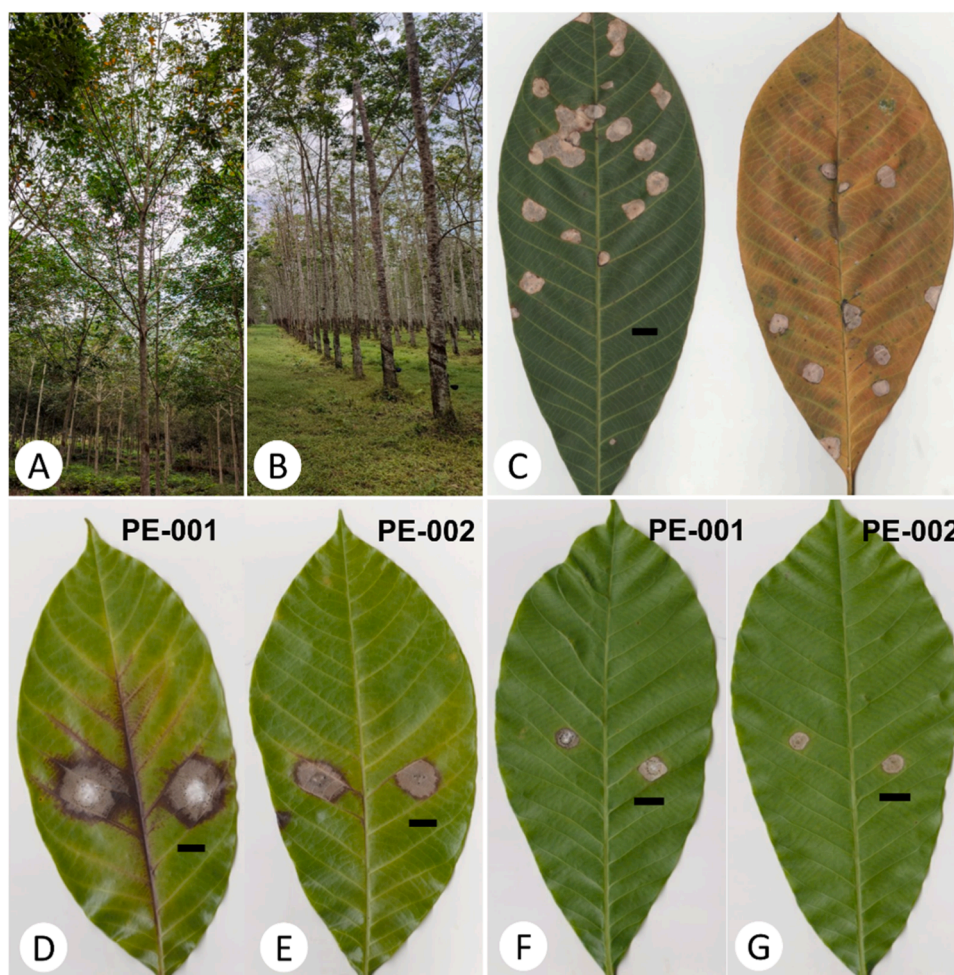
Fig. 1. Typical symptoms of circular leaf fall disease observed in the field and in bioassays following infection by *Pestalotiopsis*. Condition of the canopy of the progeny in the small-scale clone trial (A), and in a clone PB 260 field trial (B). Circular symptoms in naturally infected leaves of clone PB 260 (C). Circular symptoms in bioassay on clone PB 260 using isolates PE-001 (D) and and PE-002 (E). Circular symptoms observed in bioassay on clone SP 217 using isolates PE-001 (F) and PE-002 (G). Scale bar = 10 mm.

Table 1).

3.2. Variable diameters of lesions on the leaves of the control rubber clones and genotypes of the F1 population in bioassays

Lesion diameter distribution within the population after infection is shown in Fig. 2 and listed in Supplementary Table 2. Leaves at stage c were available for only 169 individuals of the F1 population in the budwood garden. The variation in the diameter of the lesions caused by the two *Pestalotiopsis* isolates was continuous, suggesting a typical characteristic of quantitative trait inheritance. The mean lesion diameter for the entire population of clone PE-001 was 14.51 mm while that of PE-002 was 11.48 mm. A wide range of lesion diameters was observed among the 169 rubber tree progenies. The lesion diameters measured in individual offspring ranged from 5.73 mm to 27.92 mm for PE-001 and from 3.87 mm to 26.43 for PE-002. The coefficients of variation were respectively, 15.92 % for PE-001 and 11.48 % for PE-002. Some individuals had a bigger or smaller lesion diameter than the resistant parent clone SP 217, and a bigger lesion diameter than susceptible parent clone PB 260, respectively. These results showed transgressive segregation of the lesion diameters measured for strains PE-001 and PE-002.

The lesion diameter measured in the parent clones was compared with that in the control clones, including the resistant clone RRIC 100 and the susceptible clone IRR 39 (Fig. 3). Analysis of variance (ANOVA)
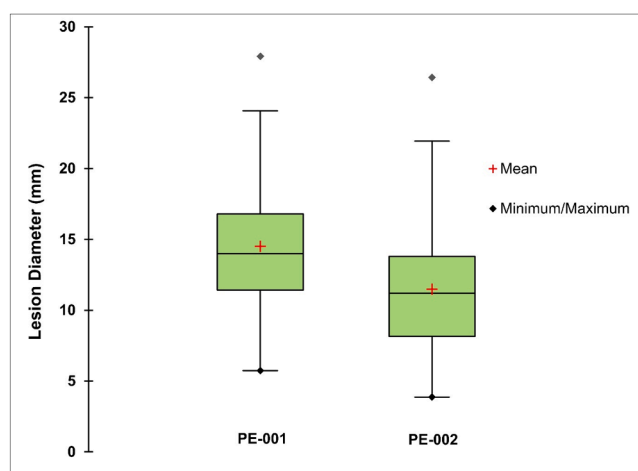
Fig. 2. Boxplot of lesion diameters (mm) measured in the rubber leaf of F1 population after inoculation with *Pestalotiopsis* isolates PE-001 and PE-002.

revealed that the values of these clones varied significantly ($P < 0.05$). The diameter of the lesion was only significantly influenced by the isolates in clones RRIC 100 and SP 217, while the diameters measured in the other clones were similar for the two isolates. Clone IRR 112 had the
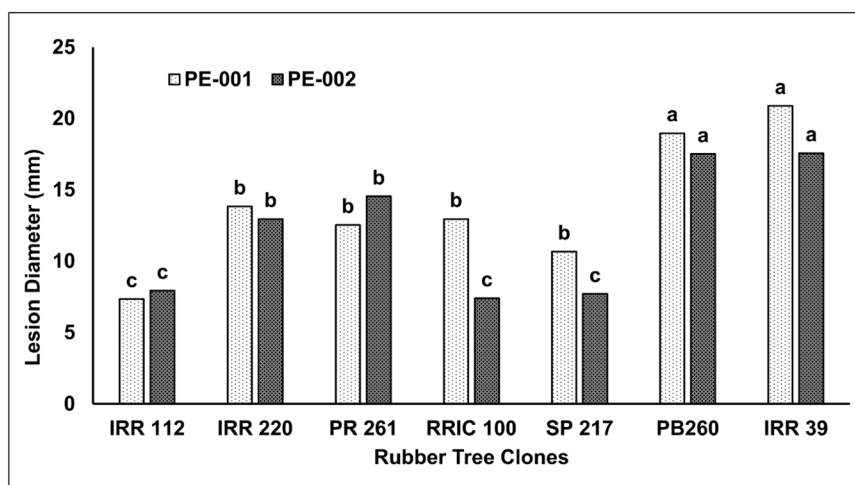
Fig. 3. Comparison of mean lesion diameters measured in the parent clones (SP 217 and PB 260) and other control clones (IRR 39, IRR 220, RRIC 100, IRR 112, PR 261) after inoculation with *Pestalotiopsis* isolates PE-001 and PE-002. The data was analysed using ANOVA and was evaluated by Scott-Knott test. Different letters in the same column indicate significantly different results of the Scott-Knott test ($p < 0.05$).

smallest lesion diameter (7.33 mm and 7.92 mm) for both isolates and clones RRIC 100 (7.39 mm) and SP 217 (7.69 mm) had the smallest lesion diameter for isolate PE-002 alone. The diameters of the lesions in clones IRR 220, PR 261, RRIC 100 and SP 217 were intermediate between that of clone IRR 112 and the highest values for clones PB 260 (18.96 mm and 17.56 mm) and IRR 39 (20.88 mm and 17.56 mm) for PE-001 and PE-002, respectively. The diameters of the lesions in parent clone SP 217 for both isolates were close to the those of the resistance clone RRIC 100 (respectively, 12.95 mm and 7.39 mm) while the diameter of the second parent clone, PB 260, was close to that of the susceptible clone, IRR 39 (20.88 mm and 17.56 mm). The average lesion diameters of the F1 progenies (14.53 mm and 11.45 mm) differed from the average of the parent clones with values situated between those of its parent clones.

3.3. Monitoring of circular disease in the small-scale clone trial (SSCT1)

Field observations were conducted when the disease incidence is usually high in the field during the rainy season (February 2020, January 2022, and March 2023), and when new leaves were formed (September 2021 and August 2022) because several leaf diseases, such as Oidium, Corynespora, and Colletotrichum, have high attacks on young leaves (stage A and B). During the field observations, the age stages of the leaves were very varied. During the observation period when new leaves were formed (September 2021 and August 2022), most of the leaves were in the A and B stages. However, during the observation periods of February 2020, January 2022 and March 2023, most of the leaves were in the C and D stages. We were not able to observe the lesion at the C stage of the leaves, but rather at the D stage.

Circular LFD occurred five times from 2017 to 2023 in the SSCT1 trial. Scoring was used to calculate disease severity (Supplementary Table 3). Disease severity was very low in February 2020 but increased at each attack and peaked in March 2023 (Fig. 4). In February 2020, the disease severity of seventy-two genotypes ranged from 3.33 % to 13.33 %, while the remaining 129 genotypes showed no disease symptoms. The same phenomenon was observed in the control clones, in which disease severity ranged from 0 % to 6.67 %. However, observations of disease severity varied on subsequent occasions, indicating differences in resistance to pathogens by each genotype in the SSCT1 trial. In 2021, disease severity ranged from 0 % to 73.33 %, whereas in the control clones, it ranged from 20 % to 41.67 %. In January and August 2022, disease severity was respectively, between 23.22 % and 80 %, and between 3.33 % and 86.67 %. In 2023, severity increased,
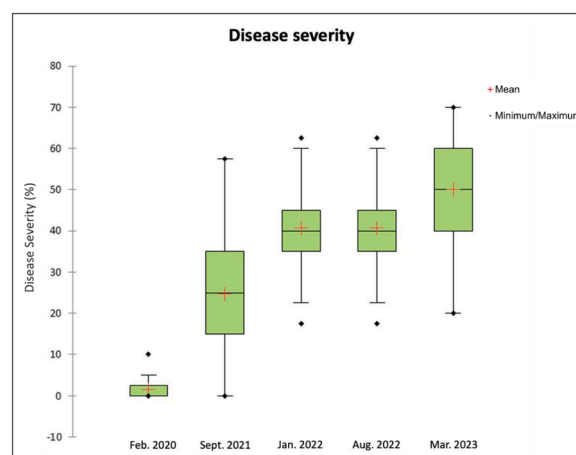

Fig. 4. Boxplot of disease severity of circular leaf fall disease in the F1 population observed at different dates during the SSCT1 trial.

ranging from 36.67 % to 93.33 %, while in the control clone, disease severity ranged from 36.67 % to 90 %. Overall, the range of disease severity in the genotypes in the SSCT1 trial was more varied, and disease severity in several genotypes was lower than that in the controls.

Disease severity in the eight control clones was calculated for the different observation dates (Fig. 5). In February 2020, disease severity in all the control clones was still very low. In some clones, severity was less than 6.67 %. In contrast, in 2020, disease incidence in the rubber plantations located around the SSCT1 trial was quite high. However, in September 2021, the severity of the disease in the control clones used in the SSCT1 trial began to increase, from 20 % in the RRIC 100 clone to 63 % in the PB 260 clone. In January 2022, disease severity again increased from 37 % in clone IRR 112–80 % in clone GT 1. In September 2020, disease severity increased slightly and did not appear to differ significantly among the rubber clones evaluated. Except for clone IRR 112, there was no change in disease severity, and the highest disease severity (70 %) was found in the PB 260 clone. In March 2023, disease severity fluctuated in each clone, ranging from 32 % in AVROS 2037, 46 % in GT1 to 90 % in RRIC 100. For most of control clones, the disease severity ranges from 60 % to 72 %. This fluctuating disease severity in each clone calls for continuing observations. Clones that have been repeatedly planted for a long time in large areas could create resistance-breaking strains that render the resistance mechanism useless.
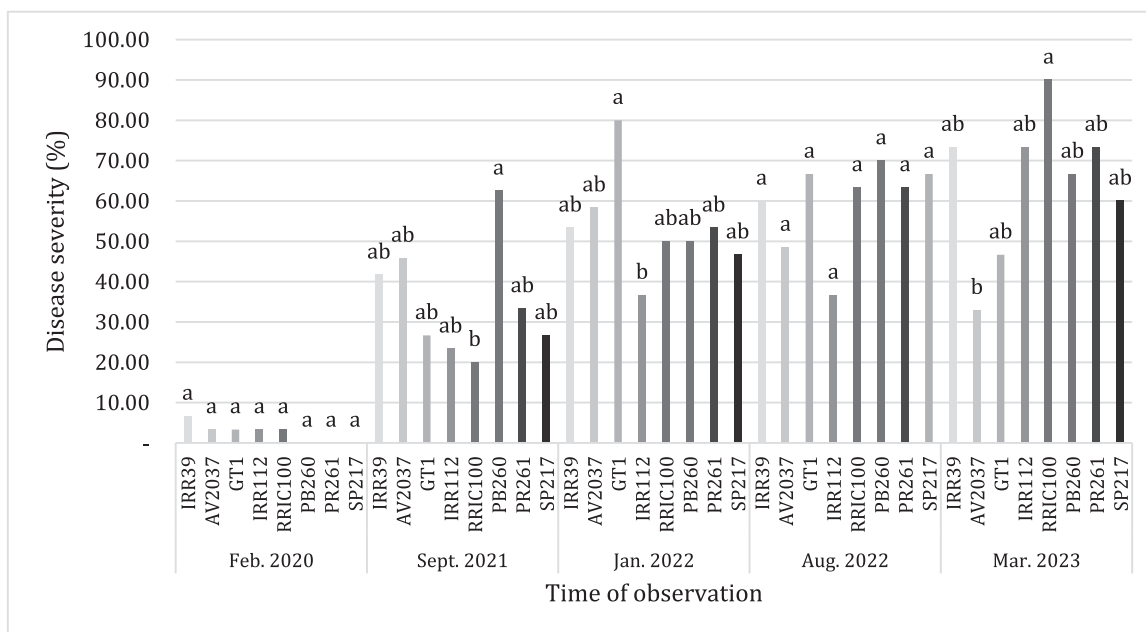
Fig. 5. Comparison of mean disease severity at different dates in parental clones (SP 217 and PB 260) and control clones (IRR 39, IRR 220, GT1, RRIC 100, IRR 112, PR 261). Different letters at the same observation date indicate significant differences (p < 0.05).

3.4. Classification of genotype according to the response to isolates in bioassays and field observations

The correlation between field observations of circular LFD at different dates and bioassays using two *Pestalotiopsis* isolates was tested using multiple linear regression. The equations are: Circular LFD-2021/9 = 2.44–0.15 x PE-001+0.04 x PE-002; Circular LFD −2022/1 = 2.61 + 0.04 x PE-001 – 0.03 x PE-002; Circular LFD −2022/8 = 3.20–0.12 x PE-001 – 0.02 x PE-002; Circular LFD −2023/3 = 3.46–0.03 x PE-001 + 0.09 x PE-002; Circular LFD-total = 2.51–0.12 x PE-001 + 0.05 x PE-002.The analysis revealed no significant correlation between field observations and bioassays (Table 1). The F values were low and had no significant p-value regardless of the date of the field observation. For the isolates PE-001 and PE-002, F ranged from 0.295 to 3.702 and from 0.088 to 2.371 for the five field observation periods, respectively.

The genotypes and parent clones were classified in four classes, using a score of 1 for the lowest to a score of 4 for the highest disease severity caused by circular LFD in the field observations or using the diameters of the lesions determined in bioassays with *Pestalotiopsis* isolates (Supplementary Table 4). The maximum class found in field observations was noted for each genotype. In the case of field observation, maximum class analysis placed no genotype in class 1, nine genotypes in class 2, twenty-one genotypes in class 3, and one hundred and sixty-five genotypes in class 4. Clone AVROS 2037 was placed in class 3, and all the other control clones were placed in class 4. Interestingly, the bioassays attributed clones SP 217 and IRR 112 to class 1 for the two isolates, RRIC 100 in class 2 and class 1 for isolates PE-001 and PE-002, clone PR 161 in class 1 and class 4 for the two isolates, and IRR 39 and PB 260 in class 4 for the two isolates.

A matrix table was built using the maximum lesion diameter classes between the two isolates and the maximum disease severity classes between the different observation dates in the SSCT1 trial (Table 2). None of the genotypes or control clones was placed in class 1 for both variables. Eight genotypes and the parent clone SP 217 were placed in class 1 concerning their lesion diameter and in class 2 for disease severity, suggesting they represent the most resistant material among the F1 population. At the opposite end of the table, thirty-eight genotypes and the control clone PR 261 were placed in class 4 for both variables. The second parent clone PB 260 and control clone IRR 39 are known to be susceptible to circular LFD, but both these clones were positioned in the

Table 2
Typology of genotypes and control clones according to the classification of disease severity made based on field observations and to the classification of lesion diameters resulting from the bioassay. The maximum classes were obtained for all the genotypes and control clones by combining the classes obtained for disease severity at different observation dates and the maximum class for lesion diameters caused by the two isolates.

		Lesion diameter			
Disease severity		Class 1	Class 2	Class 3	Class 4
Class 1		0	0	0	1
Class 2		8, SP 217	10	18	22, IRR 39, PB 260
Class 3		0	0	0	0
Class 4		14, IRR 112	27, RRIC 100	36	38, PR 261

Table 1
F and p-values of the Type III Sum of Squares analysis of the multiple linear regression (Y=PE-FO classes; X=PE-isolate test from bioassays) for the F1 progeny.

PE isolates	Linear regression parameter	Circular LFD					
		2020/2	2021/9	2022/1	2022/8	2023/3	Total
PE−001	F	-	3.702	0.706	2.591	0.295	1.679
	Pr > F	-	0.056	0.402	0.109	0.588	0.197
PE−002	F	-	0.303	0.405	0.088	2.371	0.258
	Pr > F	-	0.583	0.525	0.768	0.126	0.612

6

middle of the table (class 2 for disease severity and class 4 for lesion diameter). Clone RRIC 100, which is known to be tolerant, was placed in class 4 for disease severity and in class 2 for lesion diameter.

3.5. Analysis of heritability

Heritability was calculated using the lesion diameter observed after inoculation of two isolates in bioassays and on the severity of circular LFD monitored at different dates in the SSCT1 trial (Supplemental Table 5 and Table 3). The bioassays showed a greater heritability at family level (hf between 0.95 and 0.97) than the circular LFD (between 0.12 and 0.65).

3.6. Detection of QTLs for lesion diameter from bioassays and for disease severity from field observations

QTL analysis was carried out using BLUP data (Supplemental data 5). Apart for the residuals of the lesion diameter obtained from PE-001 isolates, all residues of lesion diameter from PE-002 (Supplemental Table 6) and disease severity calculated from the score of the field observation (Supplemental Table 7) did not follow a normal distribution (Fig. 6). Consequently, a non-parametric Kruskal-Wallis test was applied for QTL detection. Eighteen QTLs were detected and positioned on the genetic map on nine linkage groups (Fig. 7).

Four QTLs were detected for isolates PE-001 and one for PE-002 (Table 4, Supplementary Table 8). For PE-001, one QTL was located on LG1, two on LG5 and one on LG7. For PE-002, only one QTL was detected on LG5, in the same area of the two QTLs for PE-001. The K value ranged from 12.4 to 24.1 for the QTLs identified on three linkage groups (1, 5 and 7).

Thirteen QTLs were identified from field observations of the circular LFD: one on LG2, three on LG8, one on LG10, three on LG13, three on LG15, and two on LG16 (Table 5, Supplementary Table 8). Significant QTLs were detected on three out of the five observation dates: six QTLs in September 2021, one QTL in January 2022 and six QTLs in August 2022. On LG8, the three QTLs are close but do not overlap. Interestingly, no QTLs were detected in both the bioassay and field observations.

3.7. Genes underlying QTLs

Chromosomal regions underlying QTLs were identified on contigs of the genome sequence of clone PB 260 (Table 6). The size of these QTL regions ranged from 376,570 to 40,746,648 bp. The regions have a gene content ranging from 30 and 218. Interestingly, no strict correlation was found between gene content and QTL physical size. For instance, the QTL_BA_3 is the longest with 40 Mb (199 genes) while QTL_FO_4 has the most genes (218) but accounts for only 7 Mb. The frequency of Gene Ontology (GO) terms associated with the genes within the QTLs was tested over- and underrepresentation (Supplemental data 9). Depending on the chromosomal fragments linked to the QTL concerned, up to thirty-two percent of genes had a significant GO term. The most GO terms with significant GO terms were found for six QTLs: FO_7 (40 genes), FO_11 (33 genes), FO_4 and BA_3 (24 genes), FO_8 (21 genes) and GO_13 (19 genes) (Table 6). Genes were associated with under-represented GOs (95 genes) and over-represented GOs (104 genes).

Annotation of these regions revealed a large number of proteins related to cell wall synthesis and degradation, regulatory proteins including stress transduction and signalling, protein and metabolite transporters, small RNA mediated-post-transcriptional regulation, etc. (Supplemental data 10). Interestingly, the GO terms associated with the response to or defence against biotic factors all belong to the same QTL BA_5, which was found on the LG7 in the bioassay carried out with isolate PE-001 (Supplemental data 9).

4. Discussion

This first genetic study of circular LFD revealed a different genetic basis between field observations and inoculation of *Pestalotiopsis* isolates under controlled conditions. Bioassays produced a specific response to *Pestalotiopsis*, whereas field observations showed that circular LFD involves a complex mechanism linked to the environment and probably several pathogens. Genotypes were also divided into several resistance classes. This finding calls into question bioassays, field observations and breeding for tolerance to circular LFD, all of which require further elucidation.

4.1. Advantages and limitations of bioassays

In *H. brasiliensis*, the detached leaf bioassay was developed to determine the pathogenicity of several pathogens such as *Corynespora cassiicola* (Breton et al., 2000) and *Colletotrichum* spp. (Sangu and Muid, 2016). Bioassays with *Pestalotiopsis* isolates were first used by Aliya and collaborators (Aliya et al., 2022) and then by Darojat and collaborators (Darojat et al., 2023). These authors used detached leaves at stage C, knowing that leaves at stages A and B are not stable in form and are prone to wilting depending in the environmental conditions, while stage D leaves are too hard to be inoculated. In other studies, high heritability determined from the lesion diameter for both *Pestalotiopsis* isolates suggests that this bioassay methodology under controlled conditions is robust and reliable. High heritability was associated with a major QTL for lesion following inoculation of *Microcyclus ulei,* newly renamed *Pseudocercospora ulei* (Hora Júnior et al., 2014), on a large family derived from a cross with the South American Leaf Blight resistant clone MDF 180 (Le Guen et al., 2011). Conversely, a small interspecific population obtained from the *Hevea brasiliensis* × *H. benthamiana* RO 38 cultivar led to low heritability (Le Guen et al., 2007). The use of electrolyte leakage after Cassiicolin toxin treatment in the *Corynespora* bioassay showed heritabilities ranging from 0.51 to 0.79 (Tran et al., 2016).

Bioassays are tools for analysing the involvement of isolates in circular LFD. As circular LFD is presumed to involve several pathogens (Aliya et al., 2022), bioassays could help identify the role of each candidate pathogen. The two isolates in this study were identified as *Neopestalotiopsis saprophytica* for PE-001 and *Pestalotiopsis microspora* for PE-002 (Darojat et al., 2023; Kusdiana and Jamin, 2022). PE-001 was the most virulent of the four races found on the same leaf (Darojat et al., 2023). The isolate PE-001 has four QTLs on three linkage groups while PE-002 has only one QTL, revealing different defence mechanisms in line with the two species.

Although time consuming, bioassays only require simple basic equipment that can be developed in many laboratories to evaluate the resistance of plant genotypes to pathogen isolates. In the present study, the two single-spore isolates tested (PE-001 and PE-002) cannot lead to strong conclusions concerning resistance and may even lead to over-estimating resistance. Studying a variety of isolates to cover a range of plant-pathogen interaction mechanisms is needed to decipher genetic and molecular resistance mechanisms to *Pestalotiopsis* and to select resistance rubber clones. The ability to collect, store in glycerol (Maharachchikumbura et al., 2014), and test many isolates is a challenge for future studies.

While it is possible to collect isolates from different locations in

Table 3

Heritability of the different traits associated with *Pestalotiopsis* and circular LFD.

Method	PE Isolate / date	hf
Bioassay	PE−001	0.95
	PE−002	0.97
Field observations	Feb. 2020	0.12
	Sept. 2021	0.65
	Jan. 2022	0.40
	Aug. 2022	0.41
	Mar. 2023	0.33
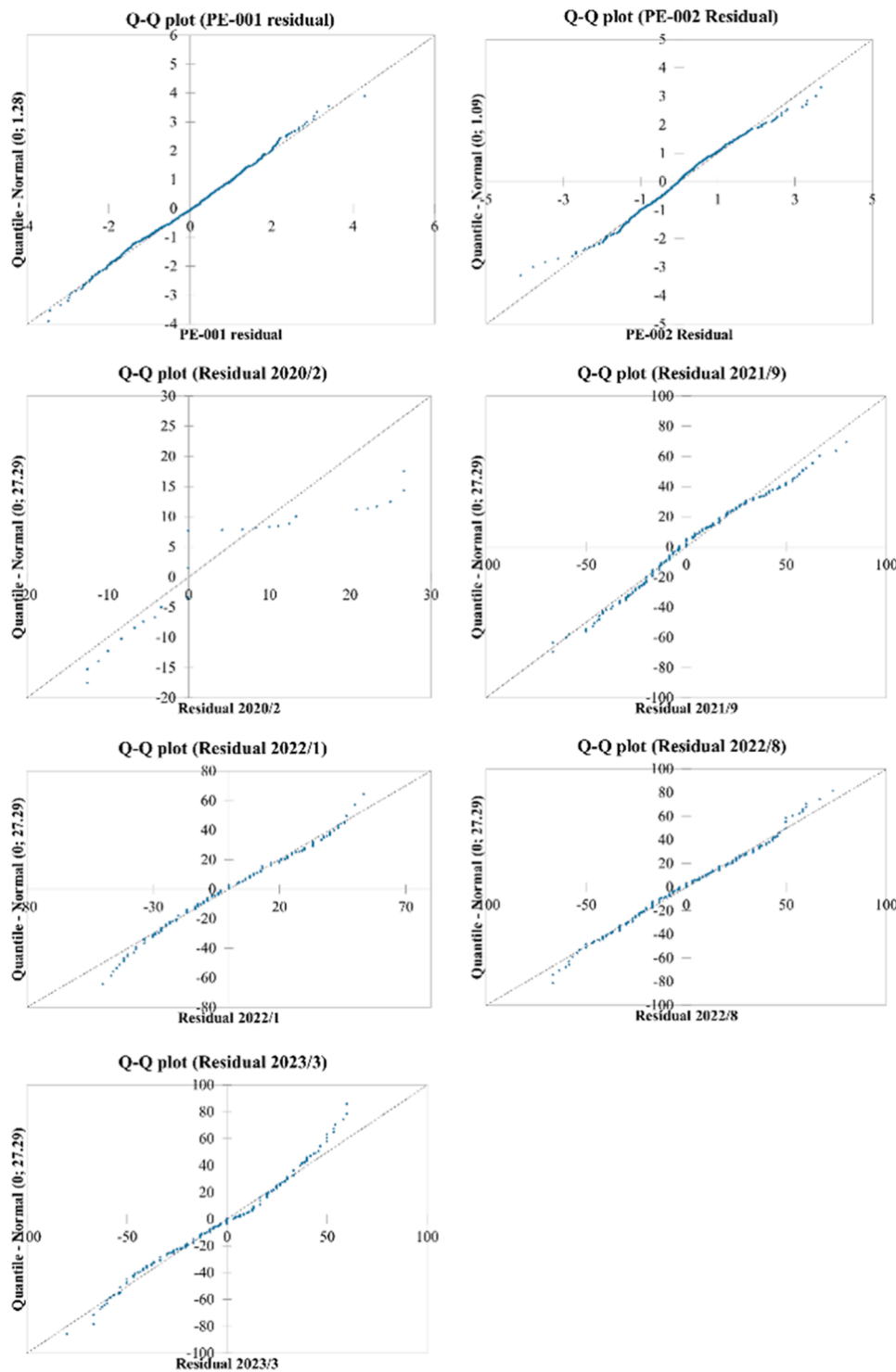
Fig. 6. Q-Q plots calculated from the lesion diameter observed in the bioassays with isolates PE-001 and PE-002 and from the disease severity observed in the field.

Indonesia, the potential introduction of dangerous pathogens from another country is strictly regulated, and recipient countries may be reluctant to agree in order to avoid any risk of dissemination. In Indonesia, regulations governing the exchange of genetic material, managed by quarantine agencies under the Ministry of Agriculture allow the transfer of dangerous pathogens affecting industrial crops only under strict control.

4.2. Field observations of circular leaf disease revealed an unstable genetic basis

Circular LFD first appeared in 2017 in North Sumatra, and then in February 2018 at the Indonesian Rubber Research Institute in South Sumatra. After a severe epidemic lasting from February to June 2018, annual epidemics have occurred, but starting in 2021, conditions have less severe than in the preceding years. The SSCT1 trial was planted in 2016 and tapped starting in January 2021. Circular LFD was first observed in this trial in February 2020, and again in September 2021,

Fig. 7. QTLs for lesion diameter observed on detached *Hevea* leaves after inoculation in bioassays with *Pestalotiopsis* i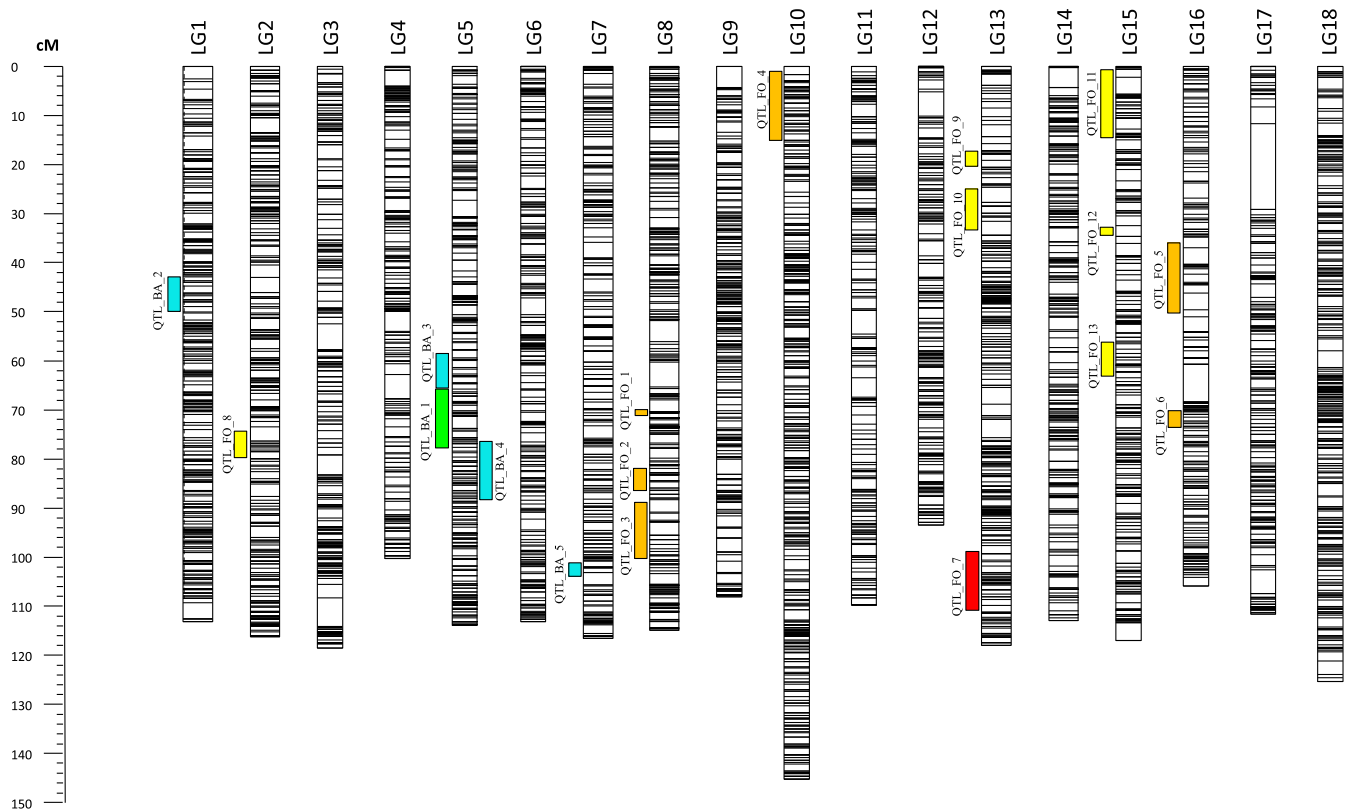solates PE-001 (QTL_BA_2–5) and PE-002 (QTL_BA_1) and for disease severity associated with circular leaf fall disease (QTL_FO_1–13) using a high-density genetic map based on a Kruskal-Wallis (K*) test. The black bars correspond to SSR and SNP markers.

Table 4

QTLs for lesion diameter observed on detached *Hevea* leaves after inoculation in bioassays with *Pestalotiopsis* isolates PE-001 and PE-002 identified using the Kruskal-Wallis test. LG: linkage group. K: Kruskall-Wallis test value.

Isolate	LG	Position	Marker	K	P-value
PE−001	1	45.416	SNP0200	12.965	0.005
	5	66.62	g5SSH42	24.139	0.00001
	5	78.588	SNP1906	17.101	0.0001
	7	104.118	SNP2706	13.022	0.0005
PE−002	5	71.029	SNP1894	12.474	0.005

January 2022, August 2022 and March 2023.

Heritability was low and varied with the dates. Heritability hf depends on the genetic variance in the population, the environment, and the accuracy of observations (Covarrubias-Pazaran, 2019). Hf ranged from 0.12 to 0.65, indicating that 12–65 % of all the phenotypic variation in the severity of circular LFD is due to variation in genotypes for that trait. This low heritability questions both strong environmental influence and the reliability of phenotyping.

The severity of the disease increased steadily over the four years of the survey. Hf was not associated with the level of infection observed in the field. However, the low heritability (0.12) determined in February 2020 could be attributed to the limited severity of the first attack of untapped trees by *Pestalotiopsis*. Only 72 genotypes were attacked by the

Table 5

Identified QTLs and K value of the Kruskal-Wallis test for disease severity associated with circular leaf fall disease observed at different dates on trees of the F1 population grown in the SSCT1 trial. LG: linkage group. Position in cM. K values in bold are significant at P-values lower than 0.005.

LG	Position	Marker	K value				
			Feb. 2020	Sept. 2021	Jan. 2022	Aug. 2022	Mar. 2023
2	75.951	SNP0578	0.096	4.569	3.394	**13.554**	0.376
8	72.324	g8A2306	5.225	**11.032**	4.996	2.302	0.009
8	85.614	SNP3097	5.546	**16.08**	4.58	3.404	3.092
8	91.119	SNP3120	1.036	**14.237**	6.64	3.746	2.712
10	8.245	SNP3683	0.269	**18.77**	0.292	0.728	2.515
13	20.392	SNP4934	0.139	0.745	0.214	**17.047**	0.35
13	34.137	SNP5022	1.328	0.02	3.062	**14.939**	0.324
13	102.961	g13A2757	1.156	1.866	**17.603**	2.202	0.617
15	10.173	SNP5737	1.471	1.158	0.104	**20.786**	0.024
15	34.651	SNP5818	0.874	0.122	2.994	**12.178**	0.149
15	63.257	SNP5917	0.788	1.418	0.786	**19.642**	0.361
16	41.802	SNP6226	7.227	**13.397**	5.084	2.86	0.213
16	71.584	SNP6355	1.586	**16.139**	0.962	3.06	2.497

Table 6
Length of QTL sequences, number of genes underlying the different QTLs, number of genes associated with gene ontology (GO) terms, and number of GO terms per QTL for lesion diameter and disease severity QTLs observed in the bioassay on detached leaves and in the SSCT1 field trial.

Type of analysis	Trait	Isolate/ Date	QTL name	LG	Contig	Length of QTL sequence (bp)	Gene (N°)	Gene with significant GO term (N°)	Under-represented GO (N°)	Under-represented gene (N°)	Over-represented GO (N°)	Over-represented gene (N°)
Bio-assay	Lesion diameter	PE−002	QTL_BA_1	5	6	29 302 673	80	8	10	6	9	2
		PE 001	QTL_BA_2	1	33	1 382 966	84	0	-	-	-	-
			QTL_BA_3	5	6	40 746 648	199	24	-	-	4	24
			QTL_BA_4	5	26	6 065 600	133	6	5	6	-	-
			QTL_BA_5	7	12	1 259 118	63	3	-	-	14	3
Field scoring	Disease severity	Sep 2021	QTL_FO_1	8	11	926 010	31	2	-	-	2	2
			QTL_FO_2	8	19	4 617 650	98	0	-	-	-	-
			QTL_FO_3	8	19	2 677 958	93	0	-	-	-	-
			QTL_FO_4	10	8	7 053 226	218	24	6	14	2	10
			QTL_FO_5	16	24	7 698 187	218	10	5	7	1	3
			QTL_FO_6	16	14	1 943 951	91	0	-	-	-	-
		Jan 2022	QTL_FO_7	13	41	1 951 100	123	40	4	17	11	23
		Aug 2022	QTL_FO_8	2	5	2 949 093	140	21	3	19	3	2
			QTL_FO_9	13	10	376 570	35	1	-	-	1	1
			QTL_FO_10	13	10	3 359 851	175	6	-	-	1	6
			QTL_FO_11	15	1	4 175 653	130	33	11	17	3	16
			QTL_FO_12	15	1	398 848	30	2	1	2	-	-
			QTL_FO_13	15	1	21 303 403	163	19	10	7	10	12

pathogen and disease severity was limited. Then, in September 2021, Hf reached 0.65, fell sharply in January (0.40) and August 2022 (0.41) when a high-intensity harvesting system was applied. Weather conditions are often considered to be the main factor influencing fungal infections. Different microclimates in neighbouring blocks may also have increased phenotype variability and affected heritability in this experiment. Weather conditions can also differ between one attack and another. Nevertheless, the harvesting system (d1 ET 2.5 % 12/y) applied starting in January 2022 is known to cause strong abiotic stress that triggers tapping panel dryness in susceptible clones and stress signalling response in latex and bark tissues (Herlinawati et al., 2022; Putranto et al., 2015a; Putranto et al., 2015b). Plant immunity is known to be controlled by abiotic factors (Pélissier et al., 2021). Therefore, the stress associated with latex harvesting needs to be carefully analysed in terms of susceptibility to foliar diseases.

The scoring method used is another possible source of variability. To reduce possible observation bias, the same observer monitored the 2080 trees used in the SSCT1 trial. The trial was monitored in the space of three days to avoid any changes in disease severity in a short space of time. Monitoring included scoring the canopy cover and observation of disease symptoms on the living leaves at a low level of the canopy. Observation of fallen leaves confirmed the symptoms observed. All leaves reached stage D. It was difficult to observe the top of the canopy. Unmanned aerial vehicle (UAV) remote sensing technology was recently used for the first time to detect powdery mildew in rubber trees (Zeng et al., 2023). Such an approach would be efficient for high-throughput phenotyping of circular LFD.

The number and position of QTLs vary over time, reflecting the complexity and diversity of the mechanisms involved. No QTL was detected when the disease first appeared in the trial. The highest number of QTLs (6) was detected in September 2021 and August 2022, during the second and fourth attacks, but was not associated with the degree of disease severity and its variance. Such QTL differences may also be related to the influence of harvesting stress (tapping and ethephon stimulation, weather conditions and the combination of biotic factors (different races, species and complexes made of different pathogens). Interestingly, QTLs were detected at a low level of hf during use of the intensive harvesting system (d1 ET 12/y). Despite the difficulties associated with observing and quantifying disease severity in the field trial, these results will help select genotypes that are more resistant to circular LFD.

4.3. Breeding for resistance to circular leaf fall disease

Resistance to circular LFD involves many genetic factors. The infection process likely requires a complex mechanism involving a first pathogen (*Colletotrichum*) to enable *Pestalotiopsis* to display its virulence (Aliya et al., 2022). No correlation between the bioassays and the field observations was found, but it is possible to select rubber clones based on the two levels of resistance determination. Eight years of field monitoring made it possible to identify the potential susceptibility of certain genotypes by using the maximum qualitative class for each genotype. For bioassays, it seems reasonable to avoid genotypes already shown to be susceptible to isolates in bioassays.

To render this approach more robust, the characterisation of a large number of isolates may improve the selection of genotypes. The combination of lesion diameter and disease severity classifications led to the identification of eight genotypes in class 1 for lesion diameter and class 2 for disease severity, suggesting a good level of resistance to circular LFD. At this stage of knowledge, breeders may suggest avoiding using the 74 genotypes belonging to class 3 or class 4 for lesion diameter or disease severity, and avoid recommending clones IRR 39, PB 260 and PR 261. Combining this classification of circular LFD resistance with other agronomic traits will be necessary in order to select rubber clones that can be recommended. Using the classification previously used for latex yield and latex diagnosis(Ismawanto et al., 2024), five high-yielding genotypes with a good classification can be identified for circular LFD.

Given the complexity of the genetic basis for resistance to circular LFD, it may be problematic to use genotypes with good resistance as the source of resistance for new crosses. *Hevea brasiliensis* is highly heterozygous and a large F1 population may include individuals with a favourable combination of genetic factors involved in resistance to circular LFD. A combination of bioassays with many isolates and several years of field observation represents a solid method for predicting the susceptibility of certain genotypes.

The identification of genes underlying QTLs is underway, opening up new prospects for the application of marker-assisted selection and a better understanding of resistance mechanisms in rubber trees. The genomic sequences corresponding to the QTLs associated to *Pestalotiopsis* and circular LFD are very long compared to sequences for traits linked to latex yield and latex diagnosis (Ismawanto et al., 2024). These long QTL regions harbour up to 218 linked genes, and their annotation revealed a panel of functions associated with plant-pathogen interaction mechanisms.

Markers associated with disease resistance and their applications in plant breeding have been particularly well developed for wheat, rice, corn and barley (Hasan et al., 2021), and also in banana (Chen et al., 2023). Quantitative resistance to disease is often partial and generally durable resistance. Many of these genes belong to the canonical resistance gene categories, with predicted functions in pathogen perception, signal transduction, phytohormone homeostasis, metabolite transport and biosynthesis, and epigenetic regulation (Gou et al., 2023). For tree species, QTL mapping has also revealed resistance genes associated with variation in leaf rust disease resistance in poplar (Nvsvrot et al., 2020), and quantitative resistance to blister rust in white pine (Weiss et al., 2020). These resistances a being associated both with R genes and with morphological and developmental processes.

5. Conclusions

This study is the first attempt to decipher the genetic basis of circular LFD. No correlation was found between the bioassays with *Pestalotiopsis* isolates and field observations. This result suggests that *Pestalotiopsis* is not the only effector of the circular leaf disease. The QTLs detected in the field at different observation dates reveal the complexity of the infection mechanism, which may involve several different pathogens and races. The high-density map of SSR and SNP markers was used to identify the long sequences underlying QTLs. These QTL regions consist of 30–218 genes, whereas only 8–48 genes were found in QTLs for yield and latex diagnosis (Ismawanto et al., 2024). These results are consistent with the observations of Aliya and colleagues, who suggest that *Colletotrichum siamense* and *Pestalotiopis jesteri* are the primary and secondary causal pathogens, respectively. The specific symptom observed in the bioassays suggests that *Pestalotiopsis* is the causal pathogen of the circular LFD in rubber leaves. This identification paves the way for further research into the resistance mechanisms and for a better understanding of this possible secondary causal pathogen.

CRediT authorship contribution statement

Sudarsono Sudarsono: Writing – review & editing, Writing – original draft, Supervision, Methodology. **Alchemi Putri Juliantika Kusdiana:** Writing – review & editing, Writing – original draft, Visualization, Validation, Resources, Methodology, Investigation, Formal analysis, Data curation. **David Lopez:** Writing – review & editing, Writing – original draft, Visualization, Validation, Resources, Methodology, Investigation, Formal analysis, Data curation. **Fetrina Oktavia:** Writing – review & editing, Writing – original draft, Supervision, Resources, Funding acquisition. **Sigit Ismawanto:** Writing – review & editing, Resources, Investigation, Formal analysis. **Pascal Montoro:** Writing – review & editing, Writing – original draft, Visualization, Validation, Supervision, Resources, Project administration, Methodology, Investigation, Funding acquisition, Formal analysis, Data curation, Conceptualization. **Muhamad- Rizqi Darojat:** Writing – review & editing, Writing – original draft, Visualization, Validation, Resources, Methodology, Investigation, Formal analysis, Data curation.

Declaration of Competing Interest

The authors declare that they have no known competing financial interests or personal relationships that could have appeared to influence the work reported in this paper.

Acknowledgments

The authors thank the Master scholarship granted to the first author, RUBIS CIRAD-UGM-IRRI Project framework supported by the LabexAgro 2011-LBX-002 coordinated by Agropolis Fondation, and acknowledge the Indonesian Rubber Research Institute for providing the location, equipment, and planting material used in this study.

Appendix A. Supporting information

Supplementary data associated with this article can be found in the online version at doi:10.1016/j.indcrop.2024.119829.

Data availability

The data are available in the supplementary data linked to this manuscript

References

Aliya, S.S.S., Nusaibah, S.A., Mahyudin, M.M., Yun, W.M., Yusop, M.R., 2022. Colletotrichum siamense and Pestalotiopsis jesteri as potential pathogens of new rubber leaf spot disease via detached leaf assay. J. Rubber Res 25, 195–212. https://doi.org/10.1007/s42464-022-00157-4.
Breton, F., Sanier, C., D'Auzac, J., 2000. Role of cassiicolin, a host-selective toxin, in pathogenicity of Corynespora cassiicola, causal agent of a leaf fall disease of Hevea. J. Rubber Res. vol.3 (n°2), 115–128.
Chaube, H.S., Singh, U.S., 1991. Plant disease management: principles and practices, Boca Raton. ed. CRC-Press, F.
Chen, A., Sun, J., Martin, G., Gray, L.-A., Hřibová, E., Christelová, P., Yahiaoui, N., Rounsley, S., Lyons, R., Batley, J., Chen, N., Hamill, S., Rai, S.K., Coin, L., Uwimana, B., D'Hont, A., Doležel, J., Edwards, D., Swennen, R., Aitken, E.A.B., 2023. Identification of a Major QTL-Controlling Resistance to the Subtropical Race 4 of Fusarium oxysporum f. sp. cubense in Musa acuminata ssp. malaccensis. Pathogens 12, 289. https://doi.org/10.3390/pathogens12020289.
Covarrubias-Pazaran, G.E., 2019. Heritability: meaning and computation, Valentin Wimmer, Emily Ziemke, Johannes Martini, Sam Storr. ed, Optimzing breeding schemes.
Cubry, P., Pujade-Renaud, V., Garcia, D., Espeout, S., Le Guen, V., Granet, F., Seguin, M., 2014. Development and characterization of a new set of 164 polymorphic EST-SSR markers for diversity and breeding studies in rubber tree (Hevea brasiliensis Müll. Arg. Plant Breed. 133, 419–426. https://doi.org/10.1111/pbr.12158.
Damiri, N., Pratama, Y., Febbiyanti, T.R., Rahim, S.E., Astuti, D.T., Purwanti, Y., 2022. Pestalotiopsis sp. infection causes leaf fall disease of new arrivals in several clones of rubber plants. Biodiversitas 23. https://doi.org/10.13057/biodiv/d230811.
Darojat, M.R., Ardhie, S.W., Oktavia, F., Sudarsono, S., 2023. New leaf fall disease in rubber-pathogen characterization and rubber clone resistance evaluation using detached leaf assay. Biodiversitas J. Biol. Divers. 24.
Fang, Y., Mei, H., Zhou, B., Xiao, X., Yang, M., Huang, Y., Long, X., Hu, S., Tang, C., 2016. De novo Transcriptome Analysis Reveals Distinct Defense Mechanisms by Young and Mature Leaves of Hevea brasiliensis (Para Rubber Tree). Sci. Rep. 6, 33151. https://doi.org/10.1038/srep33151.
Febbiyanti, T.R., 2020. Climate change and its impact on outbreak of Pestalotiopsis epidemic of Hevea in South Sumatra, in: Natural Rubber Systems and Climate Change. Presented at the FTA Working Paper, The CGIAR Research Program on Forests, Trees and Agroforestry (FTA), Palembang.
Febbiyanti, T.R., Fairuza, Z., 2019. Identifikasi penyebab kejadian luar biasa penyakit gugur daun karet di Indonesia. JPK 193–206. https://doi.org/10.22302/ppk.jpk.v37i2.616.
Febbiyanti, T.R., Kusdiana, A.P.J., Fairuzah, Z., Herlinawati, E., 2018. Outbreak Fusicoccum leaf Dis. Indones. Potential yield loss.
Febbiyanti, T.R., Tistama, R., Sarsono, Y., 2022. Karakterisasi isolat Pestalotiopsis pada karet (Hevea brasiliensis) menggunakan karakter morfologi dan molekuler. JPK 151–162. https://doi.org/10.22302/ppk.jpk.v39i2.798.
Gou, M., Balint-Kurti, P., Xu, M., Yang, Q., 2023. Quantitative disease resistance: Multifaceted players in plant defense. JIPB 65, 594–610. https://doi.org/10.1111/jipb.13419.
Guevara, A., López, M., Rivano, F., Castro, O., 2022. First report of secondary leaf fall in rubber trees caused by Phyllosticta capitalensis in the Eastern Plains of Colombia. N. Dis. Rep. 45, e12096. https://doi.org/10.1002/ndr2.12096.
Halle, F., Martin, R., 1968. ÉTUDE DE LA CROISSANCE RYTHMIQUE CHEZ L'HÉVÉA (Hevea brasiliensis Müll. Arg. EUPHORBIACÉES-CROTONOÏDÉES). Adansonia 8 (2), 475–503.
Hasan, N., Choudhary, S., Naaz, N., Sharma, N., Laskar, R.A., 2021. Recent advancements in molecular marker-assisted selection and applications in plant breeding programmes. J. Genet. Eng. Biotechnol. 19, 128. https://doi.org/10.1186/s43141-021-00231-1.
Herlinawati, E., Montoro, P., Ismawanto, S., Syafaah, A., Aji, M., Giner, M., Flori, A., Gohet, E., Oktavia, F., 2022. Dynamic analysis of Tapping Panel Dryness in Hevea brasiliensis reveals new insights on this physiological syndrome affecting latex production. Heliyon 8, e10920. https://doi.org/10.1016/j.heliyon.2022.e10920.
Hora Júnior, B.T.D., De Macedo, D.M., Barreto, R.W., Evans, H.C., Mattos, C.R.R., Maffia, L.A., Mizubuti, E.S.G., 2014. Erasing the Past: A New Identity for the Damoclean Pathogen Causing South American Leaf Blight of Rubber. PLoS ONE 9, e104750. https://doi.org/10.1371/journal.pone.0104750.
Hunter, R.E., 1983. Influence of Scab on Late Season Nut Drop of Pecans. Plant Dis. 67, 806. https://doi.org/10.1094/PD-67-806.
Ismawanto, S., Aji, M., Lopez, D., Mournet, P., Gohet, E., Syafaah, A., Bonal, F., Oktavia, F., Taryono, Subandiyah, S., Montoro, P., 2024. Genetic analysis of agronomic and physiological traits associated with latex yield revealed complex

genetic bases in Hevea brasiliensis. Heliyon 10, e33421. https://doi.org/10.1016/j.heliyon.2024.e33421.

Jones, P., Binns, D., Chang, H.-Y., Fraser, M., Li, W., McAnulla, C., McWilliam, H., Maslen, J., Mitchell, A., Nuka, G., Pesseat, S., Quinn, A.F., Sangrador-Vegas, A., Scheremetjew, M., Yong, S.-Y., Lopez, R., Hunter, S., 2014. InterProScan 5: genome-scale protein function classification. Bioinformatics 30, 1236–1240. https://doi.org/10.1093/bioinformatics/btu031.

Junaidi, J., Tistama, R., Atminingsih, A., Fairuzah, Z., Rachmawan, A., Darojat, M.R., Andriyanto, M., 2018. Fenomena gugur daun sekunder di wilayah Sumatera Utara dan pengaruhnya terhadap produksi karet. WP 37, 1–16. https://doi.org/10.22302/ppk.wp.v37i1.441.

Kent, W.J., Sugnet, C.W., Furey, T.S., Roskin, K.M., Pringle, T.H., Zahler, A.M., Haussler, D., 2002. The Human Genome Browser at UCSC. Genome Res. 12, 996–1006. https://doi.org/10.1101/gr.229102.

Kusdiana, A.P.J., Jamin, S., 2022. Impact of Pestalotiopsis leaf fall disease on leaf area index and rubber plant production. IOP Conf. Ser.: Earth Environ. Sci. 995, 012030. https://doi.org/10.1088/1755-1315/995/1/012030.

Kusdiana, A.P.J., Sinaga, M.S., Tondok, E.T., 2020. Diagnosis penyakit gugur daun karet (Hevea brasiliensis Muell. Arg.). JPK 38, 165–178. https://doi.org/10.22302/ppk.jpk.v2i38.728.

Kusdiana, A.P.J., Sinaga, M.S., Tondok, E.T., 2021. Pengaruh klon karet terhadap epidemi penyakit gugur daun *Pestalotiopsis*. War. Perkaretan 40, 41–52.

Le Guen, V., Garcia, D., Doaré, F., Mattos, C.R.R., Condina, V., Couturier, C., Chambon, A., Weber, C., Espéout, S., Seguin, M., 2011. A rubber tree's durable resistance to Microcyclus ulei is conferred by a qualitative gene and a major quantitative resistance factor. Tree Genet. Genomes 7, 877–889. https://doi.org/10.1007/s11295-011-0381-7.

Le Guen, V., Garcia, D., Mattos, C.R.R., Doaré, F., Lespinasse, D., Seguin, M., 2007. Bypassing of a polygenic *Microcyclus ulei* resistance in rubber tree, analyzed by QTL detection. N. Phytol. 173, 335–345. https://doi.org/10.1111/j.1469-8137.2006.01911.x.

Le Guen, V., Lespinasse, D., Oliver, G., Rodier-Goud, M., Pinard, F., Seguin, M., 2003. Molecular mapping of genes conferring field resistance to South American Leaf Blight (Microcyclus ulei) in rubber tree. Theor. Appl. Genet 108, 160–167. https://doi.org/10.1007/s00122-003-1407-9.

Lespinasse, D., Grivet, L., Troispoux, V., Rodier-Goud, M., Pinard, F., Seguin, M., 2000. Identification of QTLs involved in the resistance to South American leaf blight (*Microcyclus ulei*) in the rubber tree. Theor. Appl. Genet. 100, 975–984. https://doi.org/10.1007/s001220051379.

Li, H., 2018. Minimap2: pairwise alignment for nucleotide sequences. Bioinformatics 34, 3094–3100. https://doi.org/10.1093/bioinformatics/bty191.

Li, B., Liu, X., Cai, J., Feng, Y., Huang, G., 2021. First report on Neopestalotiopsis aotearoa of rubber tree in China. Plant Dis. 105, 1223. https://doi.org/10.1094/PDIS-09-20-1930-PDN.

Li, L., Yang, Q., Li, H., 2021b. Morphology, Phylogeny, and Pathogenicity of Pestalotioid Species on Camellia oleifera in China. JoF 7, 1080. https://doi.org/10.3390/jof7121080.

Li, L., Yang, Q., Li, H., 2021a. Morphology, Phylogeny, and Pathogenicity of Pestalotioid Species on Camellia oleifera in China. JoF 7, 1080. https://doi.org/10.3390/jof7121080.

Maharachchikumbura, S.S.N., Hyde, K.D., Groenewald, J.Z., Xu, J., Crous, P.W., 2014. Pestalotiopsis revisited. Stud. Mycol. 79, 121–186. https://doi.org/10.1016/j.simyco.2014.09.005.

Mournet, P., De Albuquerque, P.S.B., Alves, R.M., Silva-Werneck, J.O., Rivallan, R., Marcellino, L.H., Clément, D., 2020. A reference high-density genetic map of Theobroma grandiflorum (Willd. ex Spreng) and QTL detection for resistance to witches' broom disease (Moniliophthora perniciosa). Tree Genet. Genomes 16, 89. https://doi.org/10.1007/s11295-020-01479-3.

Nvsvrot, T., Xia, W., Xiao, Z., Zhan, C., Liu, M., Yang, X., Zhang, Y., Wang, N., 2020. Combining QTL Mapping with Genome Resequencing Identifies an Indel in an *R* Gene that is Associated with Variation in Leaf Rust Disease Resistance in Poplar. Phytopathology® 110, 900–906. https://doi.org/10.1094/PHYTO-10-19-0402-R.

Pélissier, R., Violle, C., Morel, J.-B., 2021. Plant immunity: Good fences make good neighbors? Curr. Opin. Plant Biol. 62, 102045. https://doi.org/10.1016/j.pbi.2021.102045.

Permana, E.I., Diyasti, F., 2022. Surveilans insidensi penyakit gugur daun karet *Pestalotiopsis* sp. di Provinsi Kalimantan Barat. AGROSCRIPT 4, 24–31. https://doi.org/10.36423/agroscript.v4i1.971.

Pornsuriya, C., Chairin, T., Thaochan, N., Sunpapao, A., 2020. Identification and characterization of *Neopestalotiopsis* fungi associated with a novel leaf fall disease of rubber trees (*Hevea brasiliensis*) in Thailand. J. Phytopathol. 168, 416–427. https://doi.org/10.1111/jph.12906.

Priyadarshan, P.M., 2017. Refinements to Hevea rubber breeding. Tree Genet. Genomes 13, 20. https://doi.org/10.1007/s11295-017-1101-8.

Putranto, R.A., Duan, C., Kuswanhadi, Chaidamsari, T., Rio, M., Piyatrakul, P., Herlinawati, E., Pirrello, J., Dessailly, F., Leclercq, J., Bonnot, F., Tang, C., Hu, S., Montoro, P., 2015a. Ethylene Response Factors Are Controlled by Multiple Harvesting Stresses in Hevea brasiliensis. PLoS ONE 10, e0123618. https://doi.org/10.1371/journal.pone.0123618.

Putranto, R.A., Herlinawati, E., Rio, M., Leclercq, J., Piyatrakul, P., Gohet, E., Sanier, C., Oktavia, F., Pirrello, J., Kuswanhadi, Montoro, P., 2015b. Involvement of Ethylene in the Latex Metabolism and Tapping Panel Dryness of Hevea brasiliensis. Int. J. Mol. Sci. 16, 17885–17908. https://doi.org/10.3390/ijms160817885.

Quinlan, A.R., Hall, I.M., 2010. BEDTools: a flexible suite of utilities for comparing genomic features. Bioinformatics 26, 841–842. https://doi.org/10.1093/bioinformatics/btq033.

Rodesuchit, A., 2020. The new Leaf Fall Disease in Thailand.

Sangu, S.S., Muid, S., 2016. Effects of Inoculum Concentrations of Colletotrichum gloeosporioides on Disease Development and Severity on Leaves of Rubber Tree (Hevea brasiliensis). BJRST 6, 50–54. https://doi.org/10.33736/bjrst.217.2016.

Solarte, F., Muñoz, C.G., Maharachchikumbura, S.S.N., Álvarez, E., 2018. Diversity of *Neopestalotiopsis* and *Pestalotiopsis* spp., Causal Agents of Guava Scab in Colombia. Plant Dis. 102, 49–59. https://doi.org/10.1094/PDIS-01-17-0068-RE.

Tang, C., Yang, M., Fang, Y., Luo, Y., Gao, S., Xiao, X., An, Z., Zhou, B., Zhang, B., Tan, X., Yeang, H.-Y., Qin, Y., Yang, Jianghua, Lin, Q., Mei, H., Montoro, P., Long, X., Qi, J., Hua, Y., He, Z., Sun, M., Li, W., Zeng, X., Cheng, H., Liu, Y., Yang, Jin, Tian, W., Zhuang, N., Zeng, R., Li, D., He, P., Li, Z., Zou, Z., Li, S., Li, C., Wang, J., Wei, D., Lai, C.-Q., Luo, W., Yu, J., Hu, S., Huang, H., 2016. The rubber tree genome reveals new insights into rubber production and species adaptation. Nat. Plants 2, 16073. https://doi.org/10.1038/nplants.2016.73.

Thaochan, N., Pornsuriya, C., Chairin, T., Chomnunti, P., Sunpapao, A., 2022. Morphological and molecular characterization of Calonectria foliicola associated with leaf blight on rubber tree (Hevea brasiliensis) in Thailand. J. Fungi 8. https://doi.org/10.3390/jof8100986.

Tran, D.M., Clément-Demange, A., Déon, M., Garcia, D., Le Guen, V., Clément-Vidal, A., Soumahoro, M., Masson, A., Label, P., Le, M.T., Pujade-Renaud, V., 2016. Genetic Determinism of Sensitivity to Corynespora cassiicola Exudates in Rubber Tree (Hevea brasiliensis). PLoS One 11, e0162807. https://doi.org/10.1371/journal.pone.0162807.

Weiss, M., Sniezko, R.A., Puiu, D., Crepeau, M.W., Stevens, K., Salzberg, S.L., Langley, C.H., Neale, D.B., De La Torre, A.R., 2020. Genomic basis of white pine blister rust quantitative disease resistance and its relationship with qualitative resistance. Plant J. 104, 365–376. https://doi.org/10.1111/tpj.14928.

Zeng, T., Zhang, H., Li, Y., Yin, C., Liang, Q., Fang, J., Fu, W., Wang, J., Zhang, X., 2023. Monitoring the Severity of Rubber Tree Infected with Powdery Mildew Based on UAV Multispectral Remote Sensing. Forests 14, 717. https://doi.org/10.3390/f14040717.